International Journal of Ambient Energy

ISSN: 0143-0750 (Print) 2162-8246 (Online) Journal homepage: https://www.tandfonline.com/loi/taen20

Performance Evaluation of PEM Fuel Cell- Chemical Heat Pump - Absorption Refrigerator Hybrid System

Emin Açıkkalp & Mohammad H. Ahmadi

To cite this article: Emin Açıkkalp & Mohammad H. Ahmadi (2020): Performance Evaluation of PEM Fuel Cell- Chemical Heat Pump - Absorption Refrigerator Hybrid System, International Journal of Ambient Energy, DOI: 10.1080/01430750.2020.1712238

To link to this article: https://doi.org/10.1080/01430750.2020.1712238

Publisher: Taylor & Francis & Informa UK Limited, trading as Taylor & Francis Group

Journal: *International Journal of Ambient Energy*

DOI: 10.1080/01430750.2020.1712238

Performance Evaluation of PEM Fuel Cell- Chemical Heat Pump - Absorption Refrigerator Hybrid System

Emin Açıkkalp[a,b,*], Mohammad H. Ahmadi[c]

[a]*Department of Mechanical Engineering, Engineering Faculty, Bilecik S.E. University, Bilecik, Turkey*
[b]*Bilecik S.E. University Energy Technology Application and Research Center, Bilecik S.E. University, Bilecik, Turkey*

[c]*Faculty of Mechanical Engineering, Shahrood University of Technology, Shahrood, Iran*

Abstract

The purpose of this study is to present an alternative trigeneration system consisting of proton exchange membrane fuel cell, chemical heat pump and absorption refrigeration system. The most important advantage of this system is that its fuel is hydrogen, and it is an environment-friendly system. Proton exchange membrane fuel cell is the main power and heat source; and the waste heat is utilized by means of chemical heat pump and the absorption refrigerator. Parametric investigation was performed for power output density, energy efficiency, exergy destruction rate density and the ecological function. The results were obtained numerically, and were then discussed. According to the results, the proposed system operates as environmental-friendly system in low current densities. According to the results, maximum power densities were 0.807 Wcm^{-2} at 90^{o}C and 0.772 Wcm^{-2} at 100^{o}C, and similarly, maximum energy efficiencies were 0.527 at 90^{o}C an 0.525 at 100^{o}C for the hybrid system.

*Corresponding author.
E-mail addresses: eacikkalp@gmail.com, emin.acikkalp@bilecik.edu.tr (E. Açıkkalp).

Keywords: Proton exchange membrane fuel cell, chemical heat pump, absorption refrigerator, hybrid system, trigeneration.

1. Introduction

Combined heat and power applications in which electricity and heat are produced by one fuel source have growing up in last decades. Because, this kind of energy systems enable us to use energy more efficiently. This means that one can use less fuel, and the negative environmental effects may be reduced. Especially, energy issues have gained attention owing to environmental concerns based on global warming. Another problem is the depleted fossil fuels. Renewable energy may be a solution for overcoming energy and environmental problems. Hydrogen is the most possible energy source for the future; and fuel cell technology could be a promising technology. Another promising issue for research opportunities is to utilize low temperature heat sources and energy storage technologies, especially heat storage technologies. Chemical Heat Pump (CHP) applications present possibility because heat storage systems or heating applications use low temperature heat sources. They have big advantages when compared conventional heat pumps, since they consume less electricity and provide relatively higher temperatures. Refrigeration systems can be divided into two groups which operate by electricity and are driven by thermal energy. Absorption Refrigeration (AR) systems are in the group driven by thermal energy. This thermal energy may be renewable energy (solar and geothermal), waste heat, etc. These properties make absorption refrigerators more attractive especially for the combined heat and power systems. For improving the performance of a fuel cell, Chemical Heat Pump and absorption refrigerator can be combined; and electricity, heat and cooling may be produced by using hydrogen.

In the last decade, fuel cell hybrid systems have become very popular and many studies have been conducted on this issue. At the beginning, irreversible fuel cells such as Proton Exchange Membrane Fuel Cell (PEMFC), Phosphoric Acid Fuel Cell (PAFC), Direct Carbon Fuel Cell (DAFC), Solid Oxide Fuel Cell (SOFC) and Molten Carbonate Fuel Cell (MCFC), alkaline fuel cells and peroxide fuel cells were investigated[1-5]. In these papers, operations and performances were analyzed in detail for PEMDC, PAFC, SOFC, MCFC. Fuel cell hybrid systems such as Stirling cycles [7-8] which, can

be seen that their performances are dramatically improved. Absorption refrigeration cycles [9-12] were utilized to recover heat from the fuel cells. Heat engines were investigated as bottom cycles to enhanced power output and efficiencies of the system in refs. [13-17]. Brayton cycles [14-28], and Braysson cycles [29-31] are researched for many authors as combined cycles. Thermionic generator [32] and thermally regenerative electro-chemical cycles have been studied as bottom cycles [33-35] to propose alternative solutions. In addition, fuel cell has been studied in terms of different aspects like structural design [36].

In this paper, Proton Exchange Membrane Fuel Cell-Chemical Heat Pump-Absorption Refrigerator Hybrid System (PEMFC-CHP-AR) was taken into account as an alternative trigeneration system. In the literature, to the best of the authors' knowledge, there is no system like the one considered in this study. Hybrid system is investigated for the different parameters including power density, energy efficiency, exergy destruction rate density and ecological function, which were presented by Angulo-Brown and which were improved by Yan [37, 38]. Ecological function enables a scientist or engineer to compare power output and exergy destruction; and give anyone an opportunity to design more efficient and environmental-friendly systems. Regarding these parameters, it was aimed that an alternative hybrid system is presented, and the best operation conditions are determined. Parametric investigations were carried out in the context of the study, and the obtained results were discussed.

2. System description

PEM fuel cell - CHP - AR hybrid system is presented as an alternative trigeneration system, which produces electricity, heating and cooling from one source. The system is shown in Fig. 1. The fuel of the proposed system is hydrogen. Fuel cells are devices that convert chemical energy into electricity. Another product of the fuel cells is heat output that can be utilized for some processes. PEM fuel cell is mainly composed of anode electrode, cathode electrode and a proton conducting membrane. Hydrogen is sentto the fuel cell on the anode side and it splits into two H+ ions and two electrons. The electrons are conducted through the anode and return to the cathode side of the fuel cell. On the cathode side of the fuel cell, oxygen gas forms two oxygen atoms with strong negative charge, which attracts the two H+ ions and they combine with an oxygen atom and two of the electrons from the

external circuit to form a water molecule (H_2O).In this process, electricity and heat are produced. Main reaction occurred in the fuel cell is H_2+O_2 H_2O+ electricity + heat. Rejected heat from the PEM fuel cell, which is about 100^oC, can be used in a CHP for heating processes and in an AR for the cooling processes.

CHP system is an alternative way to utilize the low temperature heat source or waste heat; and thus, the renewable energy including solar and geothermal energy can be utilized. In contrast to conventional steam-compressed heat pumps, they do not involve mechanical compression generally. In this study, i-propanol-acetone-hydrogen chemical heat pump was chosen. They have the capacity to provide heat to the environment at 150^oC-200^oC; and the operation pressure is about 1 or 2 bars. The operational process of the CHP originates from the dehydrogenation of methanol, ethanol or n-butanol and hydrogenation of formaldehyde, acetaldehyde or butyraldehyde, respectively. In these systems, the dehydrogenation reaction takes place at low-temperature (70-100^oC); and requires thermal energy; while the hydrogenation reaction is carried out at high-temperature (150-200^oC) as an exothermic reaction. The alcohol produced by the hydrogenation reaction of aldehyde or ketone and hydrogen is recycled for dehydrogenation reaction. Part of low-level thermal energy is upgraded to high-level energy; and the rest is removed by condenser at ambient temperature. No mechanical energy is necessary as a driving force[39].

Absorption refrigerator systems are the most convenient cycles to use waste heat or renewable energy similar to chemical heat pumps. The heat from the PEMFC can be utilized in an absorption refrigerator. The electricity consumption at AR can be neglected, when they are compared with mechanical compression system. NH_3 or Li-Br solutions are the most common working fluids for absorption refrigerators. Heat is provided to generator where refrigerator is vaporized, which leave as high pressure and high temperature vapor. After that, refrigerator is sent to condenser, expansion valve and evaporator, respectively; and in these processes, cooling is taken into account. Finally, refrigerant is sent to the absorber; and is absorbed by the weak solution in the absorber.

Some assumptions for the system are listed as follows:

- All components operate in steady state conditions.

- Operating pressure and temperature of the PEMFC are constant and uniform.

- Amounts of hydrogen and air are provided based on the current produced [11].

- Flow of reactants are steady, incompressible and laminar [11].

- Heat provided to CHP and AR is equal, and it is half of the removed heat from the PEMFC.

- Power input to CHP and AR is neglected.

3.Analysis

In this part, thermodynamic analysis of the hybrid system was carried out. Firstly, the analysis of PEMFC was performed. The equations of the PEMFC can be written as follows (1)- (12):

Reversible voltage is shown in Eq. (1)[11]:

$$V_o = 1.229 - 8.5\times10^{-4}\left(T - T_o\right) + 4.3085\times10^{-5} T\, ln\left(P_{H_2}\sqrt{P_{O_2}}\right) \quad (1)$$

Activation overpotential, concentration overpotential and ohmic overpotential are described in Eq. (2), Eq. (4) and Eq. (5)[22]. In Eq. (3),the exchange current density is defined[2, 11].

$$V_{act} = \left(\frac{\lambda_A + \lambda_C}{\lambda_A \lambda_C}\right)\frac{RT}{n_e F} ln\left(\frac{i}{i_o}\right) \quad (2)$$

$$i_o = 1.08\times10^{-21} e^{(0.086T)} \quad (3)$$

$$V_{con} = i\left(\beta_1(t)\frac{i}{i_m}\right)^{\beta_2} \quad (4)$$

$$V_{ohm} = \frac{i t_{mem}}{\sigma_{mem}} \quad (5)$$

where, i (Acm^{-2}) is the current density, T is the operation temperature of the fuel cell (K), T_o is the ambient temperature (K), P_{H_2} and P_{O_2} are the partial pressure of the hydrogen and oxygen (atm), α_A and α_C are the charge transfer coefficient of the anode and cathode, R is the universal gas constant ($Jmo^{-1}K$), F is the *Faraday* constant ($Cmol^{-1}$), $\beta_1$and β_2 are constants, t_{mem} (cm) and σ_{mem} ($cm\Omega^{-1}$) are the membrane thickness and membrane conductivity. The voltage of the fuel cell is (V):

$$V = V_o - V_{act} - V_{con} - V_{ohm} \tag{6}$$

The power output (W) and efficiency of the fuel cell can be calculated as in Eq. (7) and (8), respectively:

$$P_f = iVA \tag{7}$$

$$\eta_f = \frac{P_f}{-\Delta\dot{H}} \tag{8}$$

where A is the polar plate area, $-\Delta\dot{H}$ (J) is the enthalpy change or total energy provided to fuel cell per unit time; and Δh ($Jmol^{-1}$) is the molar enthalpy change at the operating temperature. $-\Delta\dot{H}$ can be described as [5]:

$$-\Delta\dot{H} = -\frac{iA\Delta h}{n_e F} \tag{9}$$

The exergy destruction rate of the fuel cell (W) is [3]:

$$ExD_f = \left(-\frac{\Delta h}{n_e F} - V_f \right) iA \tag{10}$$

The heat transfer occurred in the regenerator is [6]:

$$\dot{Q}_r = \theta_r \left(1-\varepsilon_r\right)\left(T-T_o\right) \tag{11}$$

where $\theta_r$is the heat conductance, ε_r, is theregenerator effectiveness and T_o is the ambient temperature. The heat released from the fuel cell (W) is:

$$\dot{Q}_{H,f} = -\Delta\dot{H} - P_f - \dot{Q}_r \tag{12}$$

Secondly, the equations for the CHP should be written. The heat addition (W), which happened in dehydrogenation reactor (point 3) to the CHP is written in Eq. (13)[39]:

$$\dot{Q}_{L,c} = \dot{m}_{ac}\left(\Delta H_{dr} - \Delta H_{vap(AD/K)} - \Delta H_{vap(AL)}\left(\frac{y_{AL}}{1-y_{AL}}\right)\right) \tag{13}$$

where, $\dot{m}_{ac}$ is the molar flow rate of the acetone ($mols^{-1}$), ΔH_{dr} is the enthalpy change of the dehydrogenation reaction ($Jmol^{-1}$) , $\Delta H_{vap(AD/K)}$ enthalpy change of vaporization of aldehyde or ketone ($Jmol^{-1}$), $\Delta H_{vap(AL)}$ enthalpy change of the alcohol ($Jmol^{-1}$) y_{AL} is the alcohol fraction in vapor phase .The heat rejection to the environment in hydrogenation reactor for heating process can be described in Eq. (14)[39]:

$$\dot{Q}_{H,c} = -\dot{m}_{ac}\Delta H_{hr} \tag{14}$$

where, ΔH_{hr} is the enthalpy change of hydrogenation reaction ($Jmol^{-1}$). The hydrogenation and dehydrogenation equations are expressed in Eq. (15) and (16) [39]:

$$\Delta H_{dr} = 82261.638 - 241.734T + 1.30314T^2 - 2.6713\times10^{-3}T^3 + 1.866941\times10^{-6}T^4 \quad (15)$$

$$\Delta H_{rh} = -53139.911 - 1.011T - 4.0687\times10^{-2}T^2 + 6.7723\times10^{-5}T^3 - 3.015875\times10^{-8}T^4 \quad (16)$$

enthalpy change in the vaporization process is [39]:

$$\Delta H_{vap,2(AC/P)} = \Delta H_{vap,1(AC/P)} \left[\frac{\left(1 - \frac{T_2}{T_{cr}}\right)}{\left(1 - \frac{T_1}{T_{cr}}\right)} \right]^n \quad (17)$$

where, $T_1$is the initial temperature (K), T_2 is the final temperature (K) and $T_{cr}$is the critical temperature. $\Delta H_{vap,2(AC/P)}$ (Jmol^{-1}) is the final enthalpy change of the vaporization process and $\Delta H_{vap,1(AC/P)}$ (Jmol^{1}) is the initial enthalpy change of the vaporization process. From the first law of the thermodynamics, the rejected heat from the condenser can be expressed as[40]:

$$\dot{Q}_{L,c} - \dot{Q}_{H,c} = \dot{Q}_{CON,c} \quad (18)$$

mol flow rate of the acetone can be calculated by using Eq. (19):

$$\dot{m}_{ac} = \frac{0.5\dot{Q}_{H,f}}{\left(\Delta H_{dr} - \Delta H_{vap(AD/K)} - \Delta H_{vap(A)}\left(\frac{y_A}{1-y_A}\right)\right)} \quad (19)$$

Exergy destruction rate (W) of the CHP is[30]:

$$ExD_c = T_o\left(\frac{\dot{Q}_{H,c}}{T_{H,c}} + \frac{\dot{Q}_{CON,c}}{T_{C,c}} + \frac{\dot{Q}_{L,c}}{T_{L,c}}\right) \quad (20)$$

COP of the CHP is**:**

$$\varphi_c = \frac{\dot{Q}_{H,c}}{\dot{Q}_{L,c}} \tag{21}$$

The equivalent power output of the CHP (W) is[11, 12]:

$$P_c = \dot{Q}_{H,c}\left(1 - \frac{T_o}{T_{H,c}}\right) \tag{22}$$

Equivalent efficiency of the CHP is [11,12]:

$$\eta_c = \frac{P_c}{\dot{Q}_{H,c}} \tag{23}$$

Thirdly, the analysis of the absorption refrigerator was performed using Eq. (24)-(34). The COP of the AR can be seen in Eq. (24) [11, 12]:

$$\varphi_{ab} = \frac{\dot{Q}_{L,ar}}{\dot{Q}_{G,ar}} = 0.5\left(\sqrt{\left[\left(a + \frac{I_{ar}T_o - T_{L,ar}}{C\dot{Q}_{G,ar}}\right)^2 - 4T_L\left(\frac{1}{(1+B)^2 T} - \frac{1 - I_{ar}T_o T}{C\dot{Q}_{G,ar}}\right)\right]} - \left(a + \frac{I_{ar}T_o - T_{L,ar}}{C\dot{Q}_{G,ar}}\right)\right) \tag{24}$$

where, $T_{L,ar}$ is the temperature of the cooled space of the AR, I_{ar} is the internal irreversibility parameter of the AR, a, b_1, b_2, B and K are shown in Eq. (25)-(30):

$$a = 1 + \frac{T_L - I_a B^2 T_o}{\left(1+B\right)^2 T} \tag{25}$$

$$B = \frac{\left(\sqrt{b_2} - 1\right)}{\left(1 + \sqrt{I_a b_1}\right)} \tag{26}$$

$$b_1 = \frac{\theta_{G,ar}}{\theta_{L,ar}} \tag{27}$$

$$b_2 = \frac{\theta_{G,ar}}{\theta_{L,ar}} \tag{28}$$

$$C = \frac{\left(1+B\right)^2}{A_{ar} K} \tag{29}$$

$$K = \frac{\theta_{G,ar}}{\left(1 + \sqrt{I_{ar} b_1}\right)^2} \tag{30}$$

where, $\theta_{G,r}$ $\theta_{O,ar}$ and $\theta_{L,ab}$ are heat transfer coefficient of the generator, the condenser-absorber and the evaporator, respectively. From the first law of the thermodynamics, heat rejected from the condenser is [11,12]:

$$\dot{Q}_{L,ar} + \dot{Q}_{G,ar} = \dot{Q}_{H,ar} + \dot{Q}_{A,ar} \tag{31}$$

If we define $\dot{Q}_{O,ar} = \dot{Q}_{H,ar} + \dot{Q}_{A,ar}$ Equivalent power, equivalent efficiency and exergy destruction rate of the AR is [11,12]:

$$P_{ar} = \dot{Q}_{L,ar}\left(\frac{T_{L,ar}}{T_o} - 1\right) \tag{32}$$

Energy efficiency and exergy destruction of the absorption refrigerator are;

$$\eta_{ar} = \frac{P_{ar}}{\dot{Q}_{H,ar}} \tag{33}$$

$$ExD_{ar} = T_o\left(\frac{\dot{Q}_{O,ar}}{T_o} - \frac{\dot{Q}_{H,ar}}{T} - \frac{\dot{Q}_{L,ar}}{T_{L,ar}}\right) \tag{34}$$

Finally, the power output, efficiency, exergy destruction ratio and the ecological function of the hybrid system are expressed in Eq. (35)-(38).

$$P_h = P_f + P_c + P_{ar} \tag{35}$$

$$ExD_h = ExD_f + ExD_c + ExD_{ar} \tag{36}$$

$$\eta_h = \frac{P_f + P_c + P_{ar}}{-\Delta\dot{H}} \tag{37}$$

$$E = P_f - ExD_h \tag{38}$$

4. Results and discussion

In this section, the results obtained from the considered system are presented and discussed. The system is investigated in terms of power density, energy efficiency, exergy destruction density, ecological function. Variations of these parameters are shown in Figs. 2-8 and *p*-*η*-*e* charts are drawn in Figs. 9-10. The parameters used in calculations can be seen in Table 1. The current density is the main parameter affecting the performance of the hybrid system, PEMFC, CHP and AR. To assess the performance of the hybrid system PEMFC, CHP and AR, a parametric analysis should be conducted and effects of the current density should be described. The maximum points of power output, the energy efficiency and ecological function, which are called as optimum points were found. As it is known, power output is desired to be maximum for any energy system. The higher power output means the higher energy efficiency (if the energy source is constant), and this causes to prevent the waste of energy resources. The maximum ecological function provides anyone to detect the point where difference of the power output and exergy destruction is the greatest. In the analysis, current density is changed while the others are kept constant. Mathematica software is used for calculations.

As it is seen in figs. 2 and 3, power densities of the PEMFC,CHP, AR and hybrid system are investigated in terms of current density for 90^{o}C and 100^{o}C. In Fig. 2, the changes of power densities for the hybrid system and PEMFC can be seen. For the hybrid system, the power density at 90^{o}C is bigger than the power density at 100^{o}C. The reason of this is that equivalent power density of the CHP at 100^{o}C is very smaller than the equivalent power density of the CHP at 90^{o}C. The power density of the PEMFC at 100^{o}C is bigger than the power density of the PEMFC operating at 90^{o}C, which is an expected result because power output of the PEMFC increases with temperature. Both power densities have maximum points that can be called as optimum points. For the hybrid system at 90^{o}C, the optimum power density is 0.807 Wcm^{-2} at i= 1.72 Acm^{-2} and at 100^{o}C, the optimum point of the power density is 0.772 Wcm^{-2} at i= 1.67 Acm^{-2}. The optimum points for the fuel cell at 90^{o}C and

100°C are provided at i= 1.63 Acm^{-2} and i= 1.62 Acm^{-2}, respectively. Corresponding values are 0.735 Wcm^{-2} for 100°C and 0.683 Wcm^{-2} for 90°C.

The power equivalent density variations of the CHP and AR are depicted in Fig. 3. As it is seen, AR has optimum point while CHP has not. CHP has nearly linear tendency and it increases continuously. As it can be seen and as mentioned above, the equivalent power density of the CHP at 90°C is much higher than the equivalent power density of the CHP at 100°C. It results from the chemicals used in CHP being very sensitive to temperature, especially alcohol fraction in vapor phase (*y*), and this affects performance of the CHP very dramatically.AR reaches its optimum i= 1.13 Wcm^{-2} for 90°C and its equivalent power density is equal to 0.0213 Wcm^{-2} and i=1.16 Acm^{-2} for 100°C and the equivalent power density is equal to 0.0214 Wcm^{-2}.

In Fig.4, the energy efficiency of the hybrid system and fuel cell are depicted. The hybrid system reaches its optimum point at lower current density values. For the hybrid system, the efficiency values are higher for 90°Cthan the efficiency values for 100°C after the optimum points. The reason of this is that the equivalent power of CHP density at 90°C is much bigger than the equivalent power density at 100°C of the CHP, as explained above. It reaches its optimum at i= 0.10 Acm^{-2} at 100°C and i= 0.14 Wcm^{-2} and maximum efficiency at 100°C is 0.527 and maximum efficiency at 90°C is 0.525.The efficiency of the PEMFC decreases with current density and this change is nearly linear.

The efficiencies of the AR and CHP can be seen at Fig. 5. As it is seen, CHP has constant efficiency temperature and its efficiency at 90°C is bigger than 100°C. The reason of this constant efficiency is that the efficiency of the CHP is the function of the temperature, because y is constant for any given temperature. The efficiency of the AR decreases with current, and this decreasing is logarithmic. According to these results, the current density for the hybrid system is chosen as $j_\eta < j < j_P$ for finding out optimal operation range, where j_η is the current density at maximum energy efficiency, and j_P is the current density at maximum power.

The exergy destruction densities rates are illustrated in Figs. 6 and 7. According to the results, all exergy destruction density rates rise up with current density, and all of them have similar tendency. Investigating the figures, one can say that the higher temperature and higher current density cause the higher exergy destruction density rates.

In Fig. 8., the variation of the ecological function with current density is seen. The ecological function provides anyone information about the difference power output with exergy destruction. In other words, it enables anyone to compare the useful power output and the lost power (exergy destruction). If it has positive value, this means that the power output is bigger than the exergy destruction and vice versa. When investigating the ecological function of the hybrid system, it can be seen that ecological function density at 90°C has higher values than the values at 100°C, and at higher current densities. Therefore, at higher current densities, the exergy destruction rate is bigger than the power output. The change of the ecological function is logarithmic and decreases with current density. There is an optimum (maximum) point for the ecological function for the hybrid system at 90°C where it is provided at i= 0.1 Acm^{-2}. There is no optimal point for the hybrid system at 100°C; however, maximum points in this condition are provided of the beginning point of the considered operation range (i= 0.07 Acm^{-2}).

Finally, P-η-E curves of the hybrid system for 90°C and 100°C are illustrated in Figs.9-10, where E_{max} is the maximum ecological function, E_P is the ecological function at the maximum power output, E_η is the ecological function at the maximum efficiency, P_{max} is the maximum power output, P_η is the power output at the maximum efficiency, P_E is the power output at the maximum ecological function, η_{max} represents the maximum efficiency and η_P represents efficiency at the maximum output. In Fig. 9, the results at 90°C can be seen. According to the results, E_P is -1.181 Wcm^{-2}and the maximum ecological function, which is the value at minimum current density (j=0.07 Acm^{-2}), is equal to 0.0024 Wcm^{-2}. E_η is 95% of the maximum ecological function. η_P is 60 % of the maximum efficiency and P_η is equal to 13% of the maximum power density. P_E is equal to 7% of the maximum power output and η_E is nearly 98% of the maximum efficiency.

The results at 100°C is shown in Fig. 10.E_P is -1.166 Wcm^{-2} and the maximum ecological function is equal to 0.005 Wm^{-2}. E_η is -0.0013 Wcm^{-2}. η_P is 59% of maximum efficiency and P_η is equal to 12% of maximum power density.P_E is 10% of maximum power output, $\eta_E$is nearly equal to maximum efficiency.

5. Conclusions

In this study, the PEMFC-CHP-AR hybrid system was investigated. In the model founded, all irreversibilities including electrochemical ones are taken into account. Equivalent power and efficiencies of the CHP and AR were derived. The power density, exergy destruction density, energy efficiencies and ecological function were chosen as performance parameters and these were researched. Maximum or minimum values were defined as if they existed. According to the results, it was determined that bigger power output is obtained from the hybrid system at 90^{o}C than the power output at 100^{o}C. The same result is true for the energy efficiency of the hybrid system. In terms of power outputs, maximum points or higher power outputs are obtained at current densities between 1-2 Am^{-2}. In contrast, higher energy efficiencies are provided at low current densities. When exergy destruction rates are researched, it can be seen that exergy destruction rates, which is the lost power in any system, have lower values at lower current densities. In addition, exergy destruction rates of hybrid system operating at 90^{o}C is smaller than the exergy destruction rates at 100^{o}C. Finally, when ecological function is checked, it is seen that lower current density values have bigger ecological function values. The importance of the ecological function is that it enables anyone to compare power output and exergy destruction rate (lost power), as it is explained above.

According to the results, it is shown that higher power output can be provided at higher current densities. However, at these current densities, the hybrid system has smaller energy efficiency and ecological function, while exergy destruction rates have bigger values. For more environmentally efficient usage of the hybrid system, it should be used under conditions of $i_E<i<i_\eta$where i_E, which are the current densities at maximum ecological function; and i_η is the current density of the maximum efficiency. For future studies, it can be recommended that economical or thermo-economical evaluation of the hybrid system is investigated, and obtained results may be compared with the results presented in this study.

Conflict of interest

There is no conflict of interest

References

[1] Zhao Y., Ou C, Chen J, A new analytical approach to model and evaluate the performance of a class of irreversible fuel cells, International Journal of Hydrogen Energy 33 (2008) 4161 – 4170.

[2] Zhang X, Guo J, Chen J, The parametric optimum analysis of a proton exchange membrane (PEM) fuel cell and its load matching, Energy 35 (2010) 5294-5299.

[3] Zhang H, Lin G, Chen J, Performance analysis and multi-objective optimization of a new molten carbonate fuel cell system, International Journal of Hydrogen Energy 36 (2011) 4015 – 4021.

[4] Zhang H, Chen L, Zhang J, Chen J, Performance analysis of a direct carbon fuel cell with molten carbonate electrolyte, Energy 68 (2014) 1-9.

[5] Zhang H, Lin G, Chen J, Multi-objective optimization analysis and load matching of a phosphoric acid fuel cell system, International Journal of Hydrogen Energy 37 (2012) 3438-3446.

[6] Chen L, Zhang H,Gao S, Yan H, Performance optimum analysis of an irreversible molten carbonate fuel cell - Stirling heat engine hybrid system, Energy 64 (2014) 923-930.

[7] Chen L, Gao S, Zhang H, Performance Analysis and Multi-Objective Optimization of an Irreversible Solid Oxide Fuel Cell-Stirling Heat Engine Hybrid System, *Int. J. Electrochem. Sci.,* 8 (2013)10772 - 10787.

[8]Açıkkalp E., Thermo-environmental performance analysis of irreversible solid oxide fuel cell – Stirling heat engine, International Journal of Ambient Energy, article in press DOI: 10.1080/01430750.2017.1345011.

[9] Yang P, Zhang H, Hu Z, Parametric study of a hybrid system integrating a phosphoric acid fuel cell with an absorption refrigerator for cooling purposes, International Journal of Hydrogen Energy 41 (2016) 3579 -3590.

[10] Chen X , Wang Y, Zahao Y, Zhou Y, A study of double functions and load matching of a phosphoric acid fuel cell/heat-driven refrigerator hybrid system, Energy 101 (2016) 359-365.

[11] Yang P, Zhang H, Parametric analysis of an irreversible proton exchange membrane fuel cell/absorption refrigerator hybrid system, Energy 85 (2015) 458-467.

[12]Zhang H, Chen X., Lin B, Chen J, Maximum equivalent efficiency and power output of a PEM fuel cell/refrigeration cycle hybrid system, International Journal of Hydrogen Energy 36 (2011) 219 0-2196.

[13] Zhao Y, Chen J, Modeling and optimization of a typical fuel cell–heat engine hybrid system and its parametric design criteria, Journal of Power Sources 186 (2009) 96–103.

[14] Zhang H, Lin G, Chen J, Performance Evaluation and Parametric Optimum Criteria of an Irreversible Molten Carbonate Fuel Cell-Heat Engine Hybrid System, *Int. J. Electrochem. Sci.* 6 (2011) 4714 - 4729.

[15] Zhang X, Chen J, Performance analysis and parametric optimum criteria of a class of irreversible fuel cell/heat engine hybrid systems, International Journal of Hydrogen Energy 35 (2010) 284 – 293.

[16] Zhang X,Wang Y, Guo J, Shih T-M, Chen J, A unified model of high-temperature fuel-cell heat engine hybrid systems and analyses of its optimum performances, International Journal of Hydrogen Energy 39 (2014) 1811 –1825.

[17]Açıkkalp E., Ecologic and Sustainable Objective Performance Analysis of Molten Carbonate Fuel Cell - Heat Engine Hybrid System, Journal of Energy Engineering 143 (6) (2017)

[18] Zhang X, Su S, Chen J, Zhao Y, Brandon N, A new analytical approach to evaluate and optimize the performance of an irreversible solid oxide fuel cell-gas turbine hybrid system, International Journal of Hydrogen Energy 36 (2011) 15304 –15312.

[19] Haseli H, Dincer I, Naterer GF, Thermodynamic analysis of a combined gas turbine power system with a solid oxide fuel cell through exergy, ThermochimicaActa 480 (2008) 1–9

[20] Açıkkalp E., Ecologic and Sustainable Objective Thermodynamic Evaluation of Molten Carbonate Fuel Cell - Supercritical CO_2 Brayton Cycle Hybrid System, International Journal of Hydrogen Energy 42 (2017) 6272-6280.

[21] HaseliH, Dincer I, Naterer GF, Thermodynamic modeling of a gas turbine cycle combined with a solid oxide fuel cell, International Journal of Hydrogen Energy 33 (2008) 5811 –5822.

[22] Açıkkalp E., Performance analysis of irreversible solid oxide fuel cell – Brayton heat engine with ecological based thermo-environmental criterion, Energy Conversion and Management, 148 (2017) 279-286

[23] Zhang X, Guo J, Chen J, Influence of multiple irreversible losses on the performance of a molten carbonate fuel cell-gas turbine hybrid system, International Journal of Hydrogen Energy 37 (2012) 8664 –8671.

[24] D. Sánchez, R. Chacartegui, F. Jiménez-Espadafor, T. Sánchez, A new concept for high temperature fuel cell hybrid systems using supercritical carbon dioxide, J. Fuel Cell Sci. Technol 6 (2009) 021306.

[25] D. Sanchez, J.M. Munoz de Escalona, R. Chacartegui, A. Munoz, T. Sanchez, A comparison between molten carbonate fuel cells based hybrid systems using air and supercritical carbon dioxide Brayton cycles with state of the art technology, Journal of Power Sources 196 (2011) 4347–4354.

[26] Zhang X, Liu H, Ni M, Chen J, Performance evaluation and parametric optimum design of a syngas molten carbonate fuel cell and gas turbine hybrid system, Renewable Energy 80 (2015) 407-414.

[27] MehrpooyaM. ,Bahramian P., Pourfayaz F. , Rosen M.A., Introducing and analysis of a hybrid molten carbonate fuel cell-supercritical carbon dioxide Brayton cycle system, Sustainable Energy Technologies and Assessments 18 (2016) 100–106.

[28] Jokar M. A., Ahmadi H. A.,Sharipfur M., Meyer J. P., Pourfayaz F., Ming T., Thermodynamic evaluation and multi-objective optimization of molten carbonate fuel cell-supercritical CO_2 Brayton cycle hybrid system, Energy Conversion and Management 153 (2017) 538–556.

[29] Zhang H, Su S, Lin G, Chen J, Performance Analysis and Multi-Objective Optimization of a Molten Carbonate Fuel Cell Braysson Heat Engine Hybrid System, *Int. J. Electrochem. Sci.* 7 (2012)3420 - 3435.

[30] Açıkkalp E., Performance analysis of irreversible molten carbonate fuel cell – Braysson heat engine with ecological objective approach, Energy Conversion and Management 132 (2017) 432–437.

[31] Ahmadi M.H., Jokar M.A., Ming T., Feidt M., Pourfayaz F., Astaraei F.R., Multi-objective performance optimization of irreversible molten carbonate fuel cell-Braysson heat engine and thermodynamic analysis with ecological objective approach. Energy 144 (2018) 707-722.

[32] Huang C, Pan Y, Wang Y, Su G, Chen J, An efficient hybrid system using a thermionic generator to harvest waste heat from a reforming molten carbonate fuel cell, Energy Conversion and Management 121 (2016) 186–193.

[33] Long R., Li B., Liu Z., Liu W., A hybrid system using a regenerative electrochemical cycle to harvest waste heat from the proton exchange membrane fuel cell, Energy 93 (2015) 2079-2086.

[34] Zhang X. , Pan Y. , Cai L. , Zhao Y. , Chen J., Using electrochemical cycles to efficiently exploit the waste heat from a proton exchange membrane fuel cell, Energy Conversion and Management 144 (2017) 217–223.

[35] Zhang X. , Cai L. , Liao T. , Zhou Y. , Zhao Y. , Chen J., Exploiting the waste heat from an alkaline fuel cell via electrochemical cycles, Energy 142 (2018) 983-990.

[36] Huijun F, Lingen C, Zhihui X, Fengrui S. Constructal optimization for a single tubular solid oxide fuel cell. J Power Sources 2015;286:406–13.

[37] Angulo-Brown F., An ecological optimization criterion for finite-time heat engines, Journal of Applied Physic, 69, 7465-7469, 1991.

[38] Yan Z., Comment on Ecological optimization criterion for finite-time heat-engines, Journal of Applied Physic, 73, 3583, 1993.

[39] Karaca F., Kıncay O., Bolat E., Economic analysis and comparison of chemical heat pump systems, Applied Thermal Engineering 22 (2002) 1789–1799.

[40] Kim T.G., Yoo Y K, SongH K,Chemıcal Heat Pump Based on Dehydrogenatıon and Hydrogenatıon of I-Propanol and Acetone, Internatıonal Journal of Energy Research, Vol. 16 (1992) 897-916.

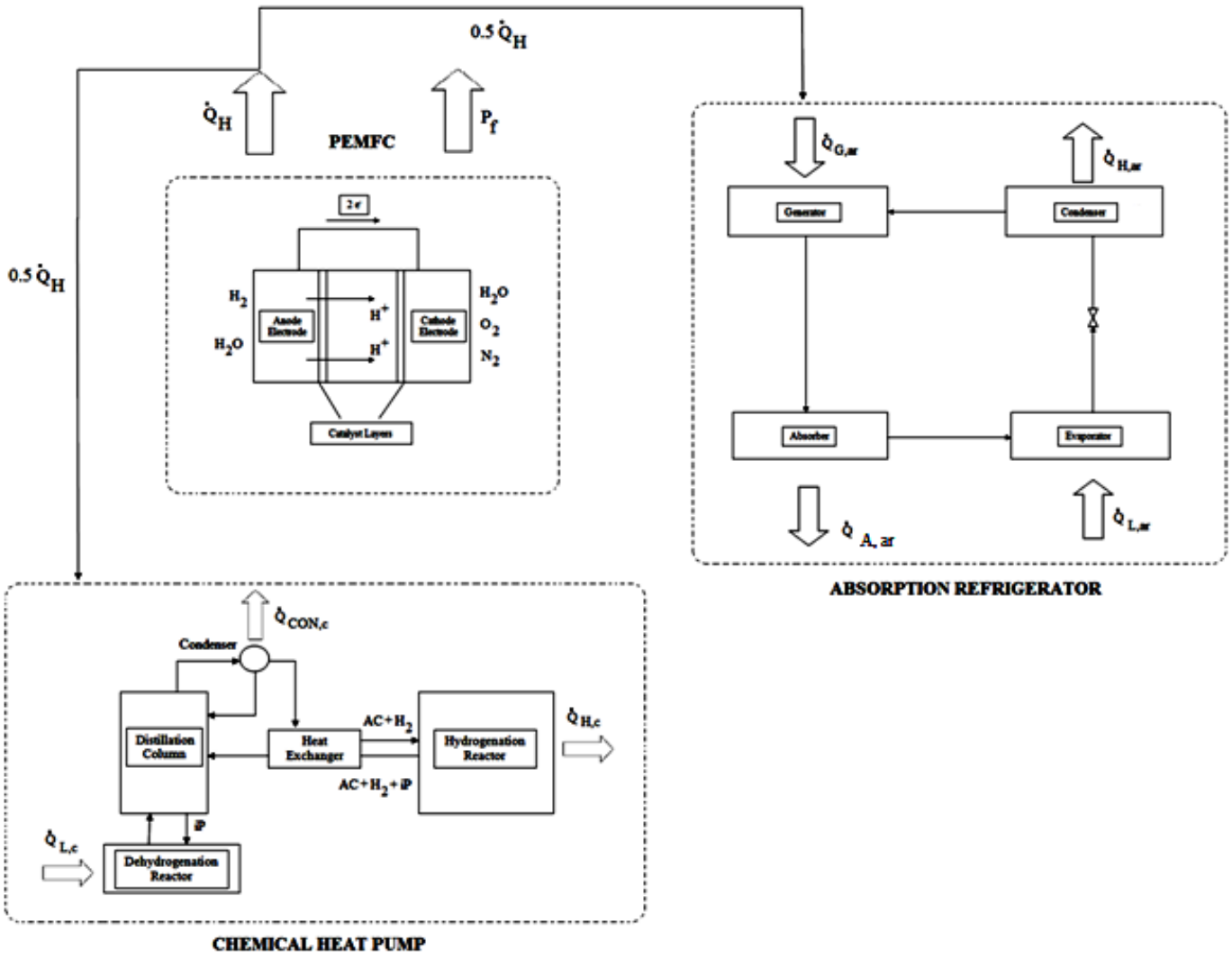

Fig.1. Schematic of the system.

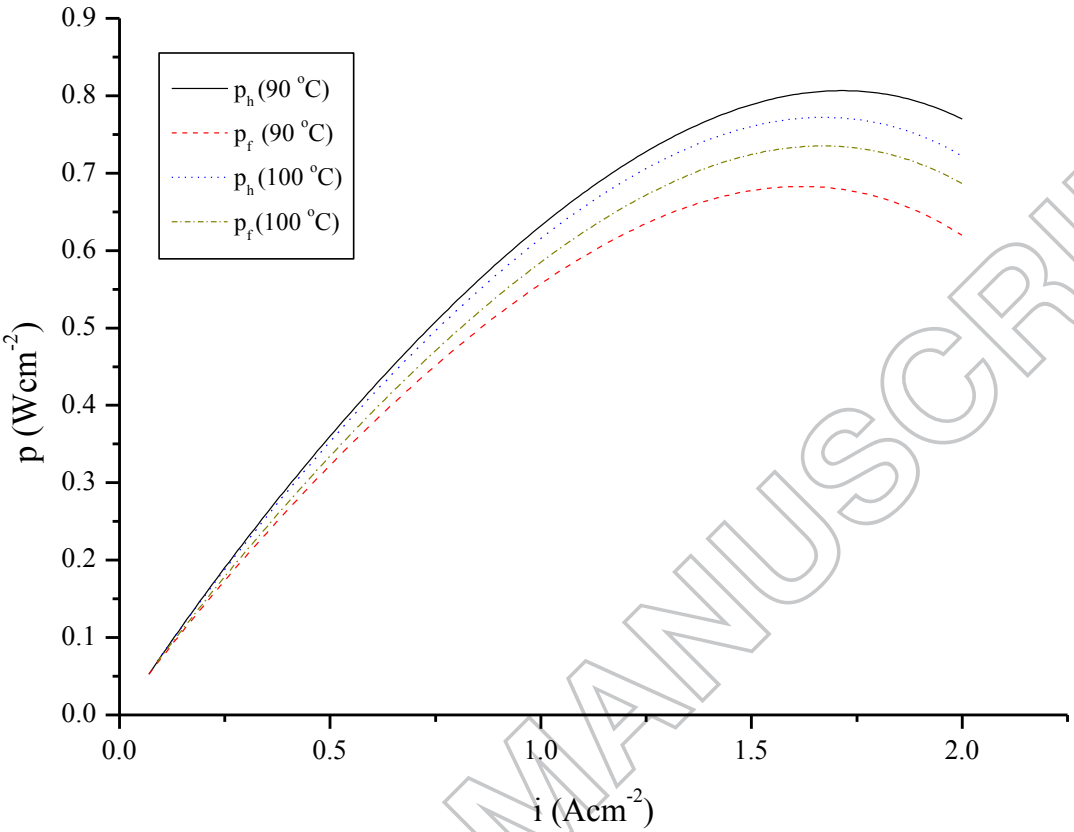

Fig. 2. Change of power densities of PEMFC and hybrid system.

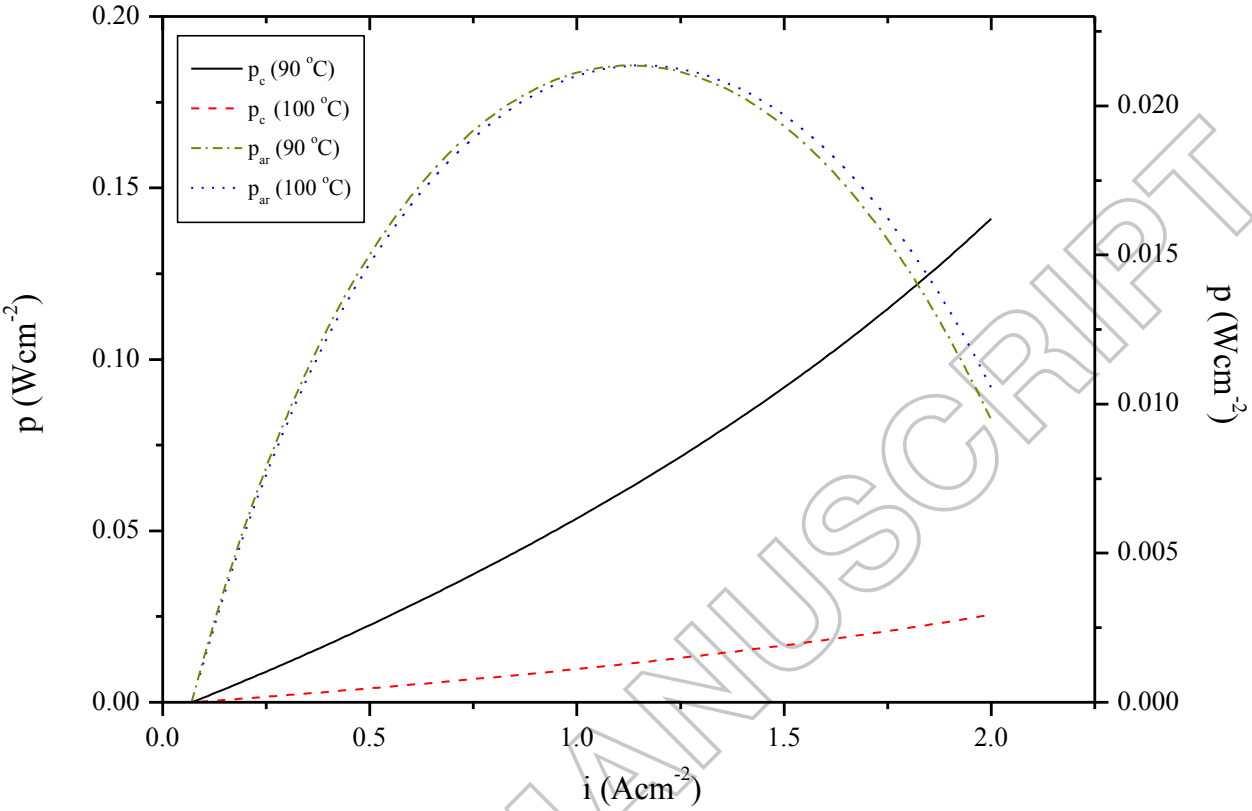

Fig. 3. Change of equivalent power densities of CHP and AR.

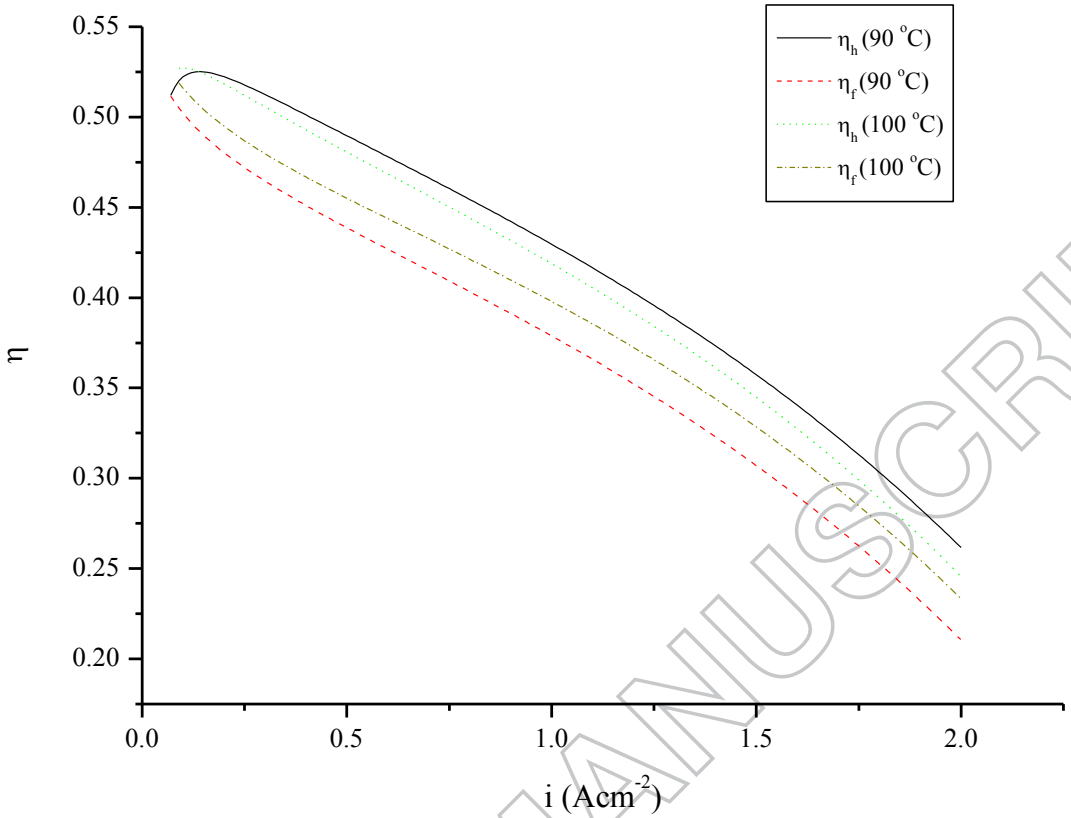

Fig. 4. Change of energy efficiencies of thePEMFC and thehybrid system.

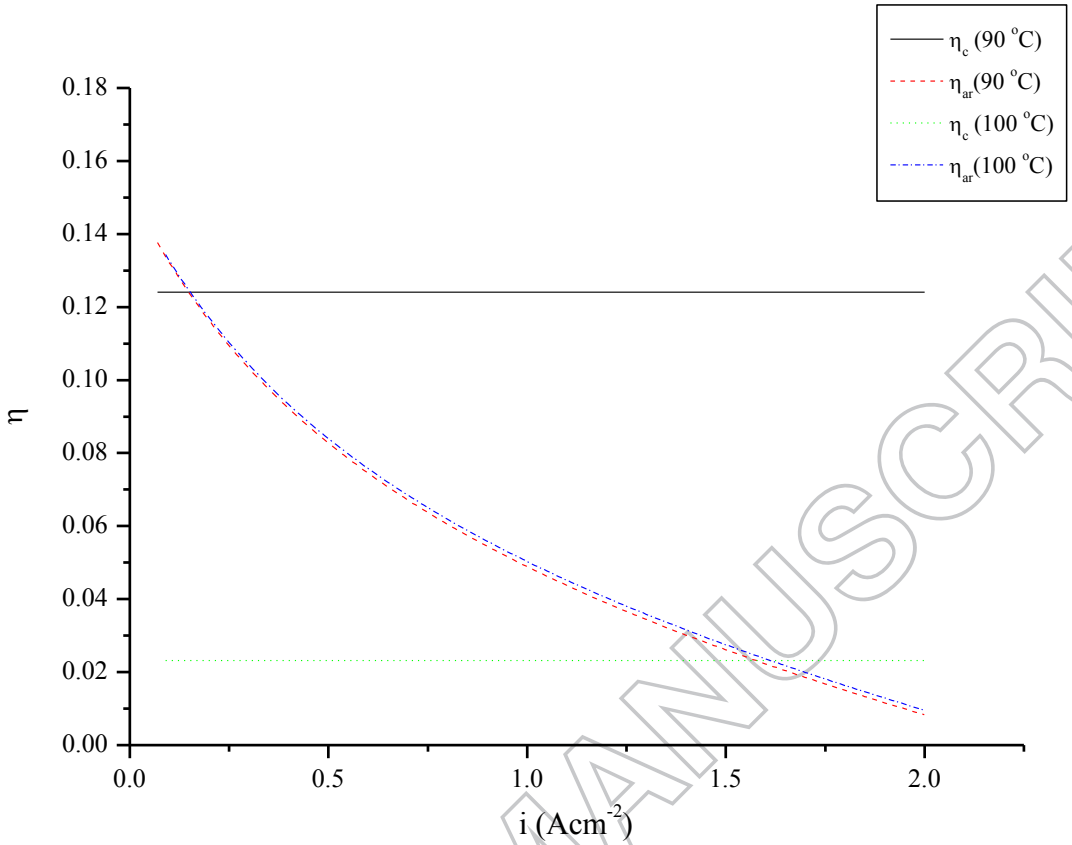

Fig. 5. Change of the energy efficiencies of CHP and AR

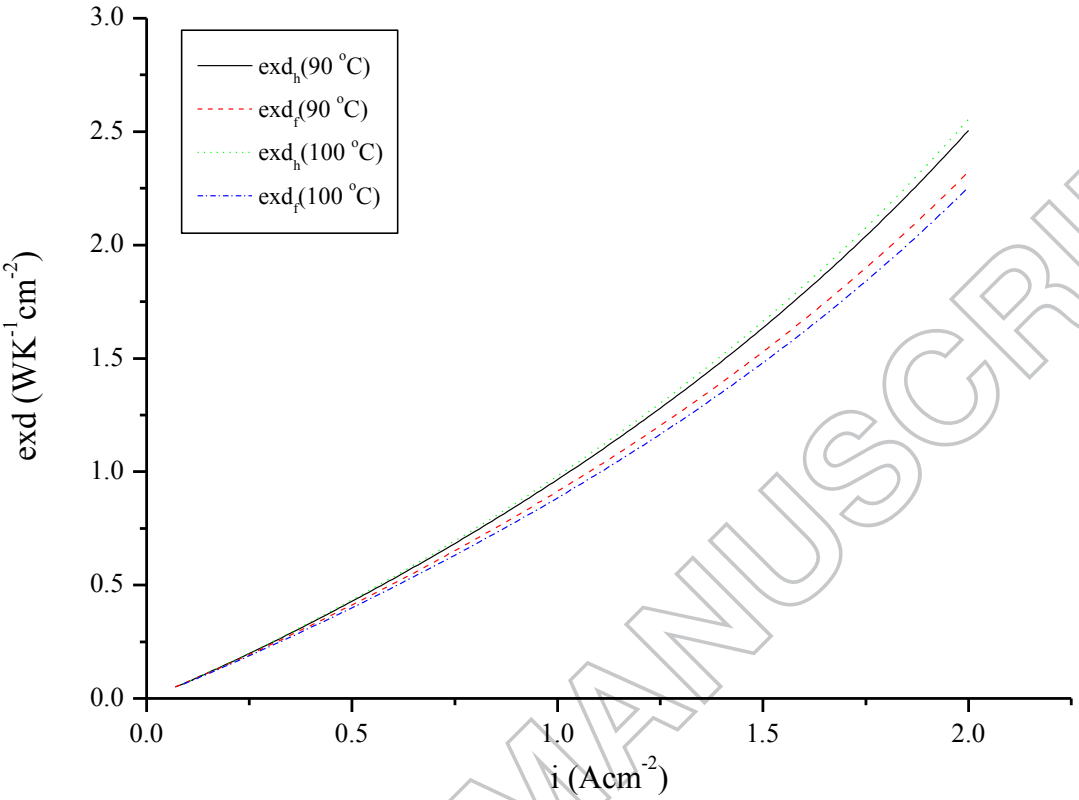

Fig. 6. Change of the exergy destruction densities of PEMFC and hybrid system.

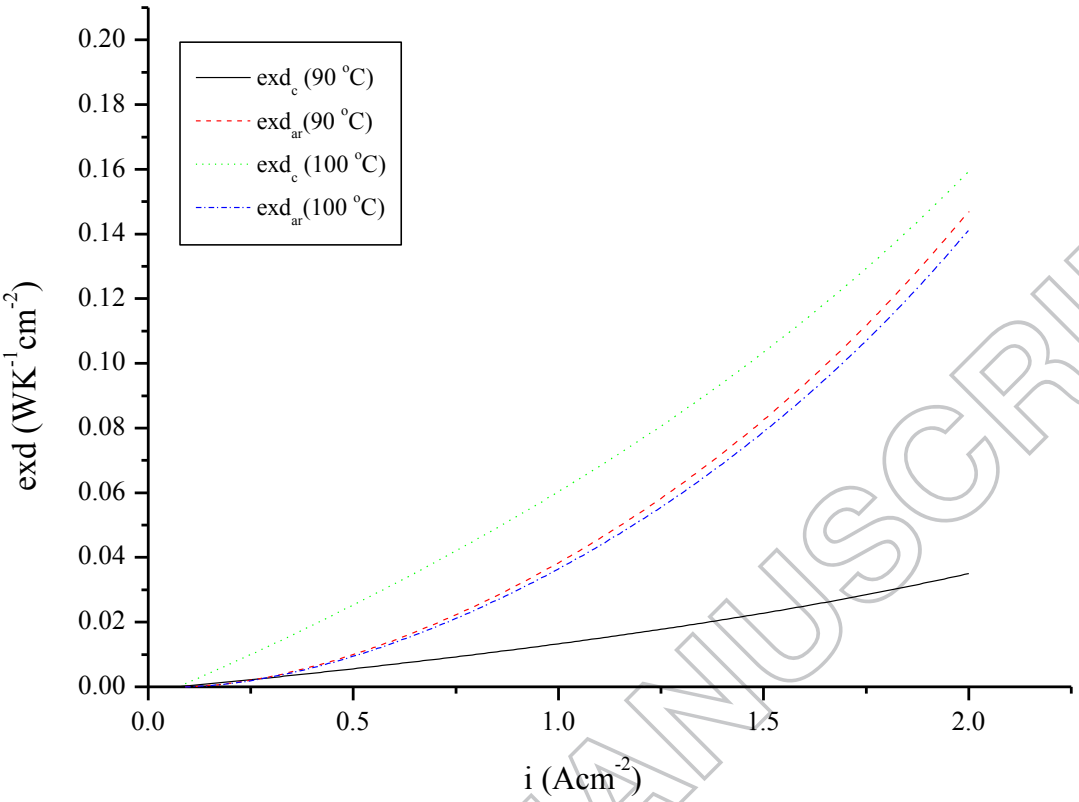

Fig. 7. Change of the exergy destruction densities of CHP and AR.

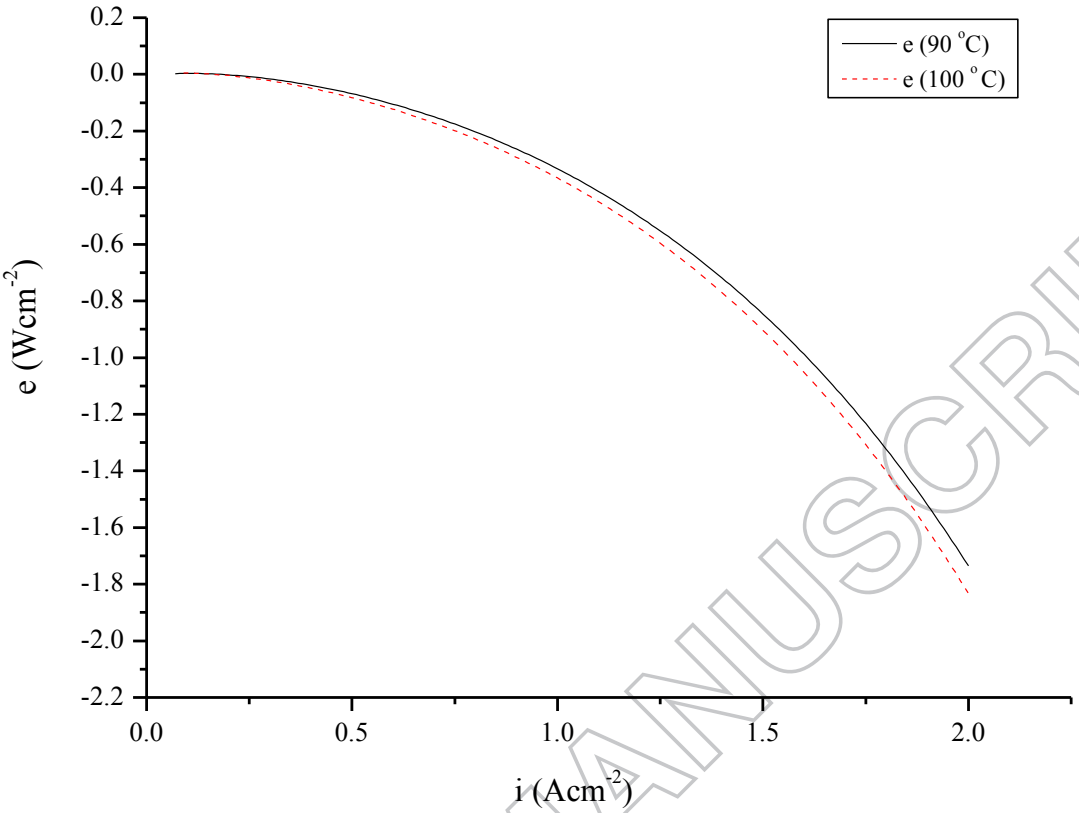

Fig. 8. Change of ecological function of the hybrid system.

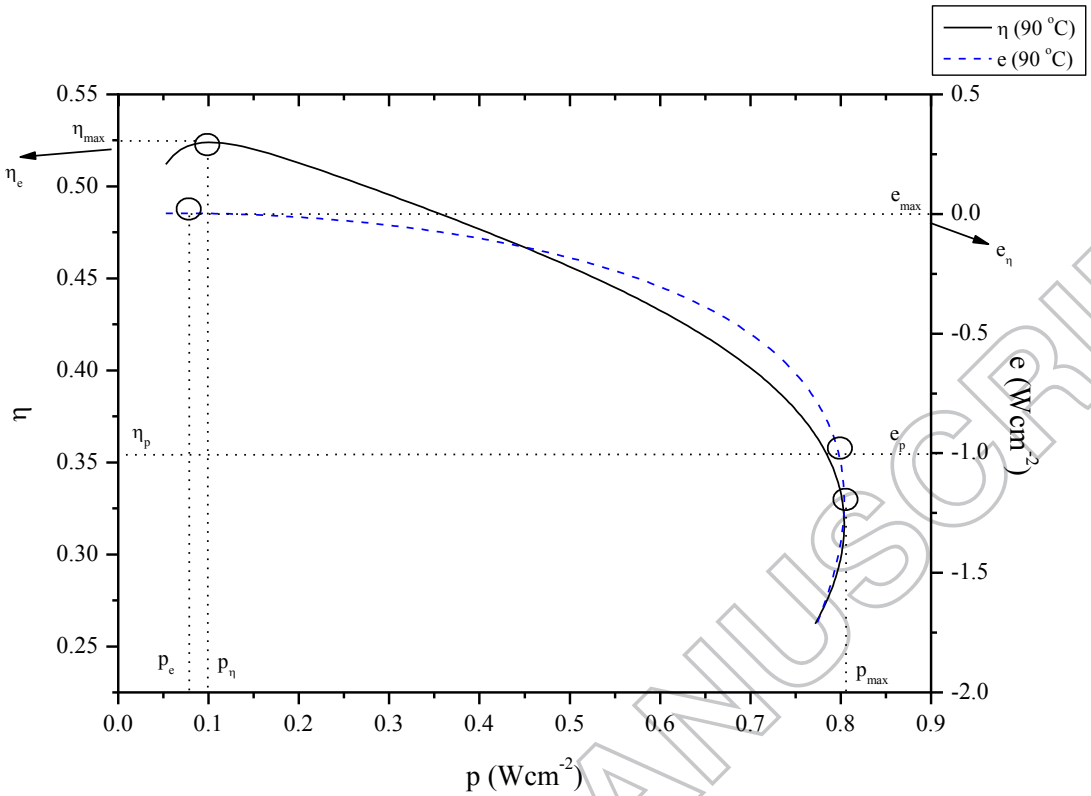

Fig. 9. *P-η-E* curve of the hybrid system at 90°C.

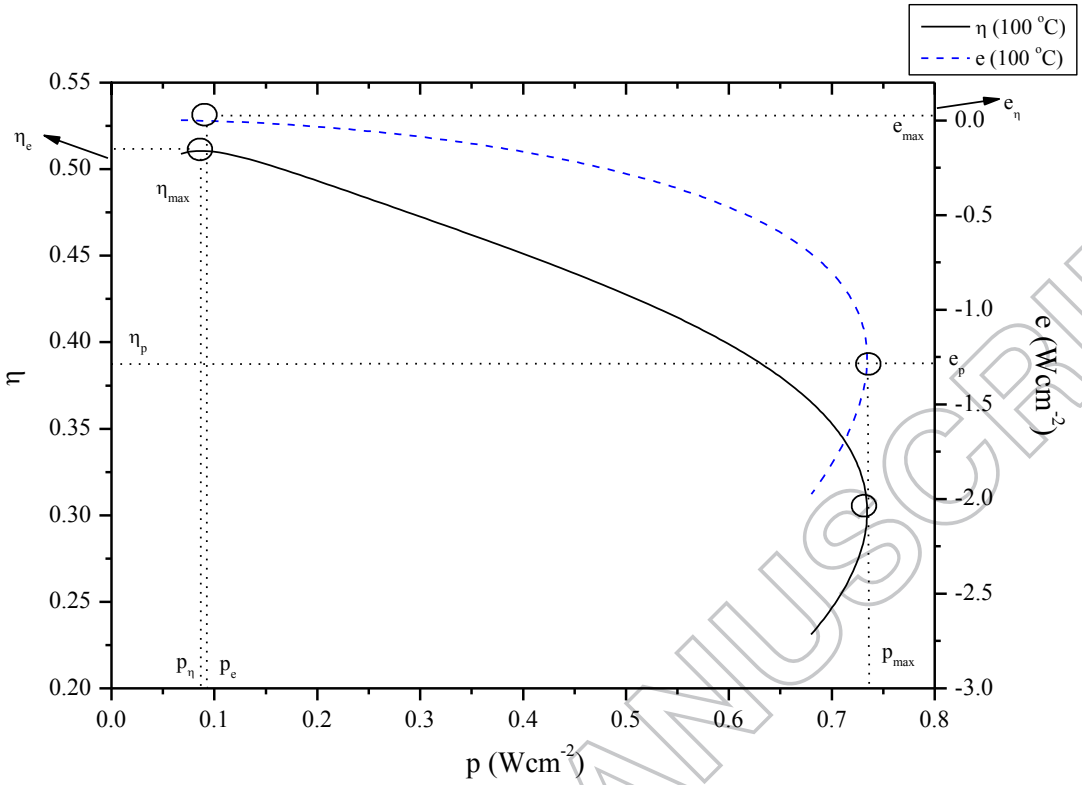

Fig. 10. *P-η-E* curve of the hybrid system at 100°C.

Table 1. Values used in calculations [12, 40].

Parameter	*Unit*	*Value*
n_e	-	2
F	C mol^{-1}	96485
Δg^o	J mol^{-1}	-237300
t_{mem}	cm	0.018
R	J $mol^{-1}K^{-1}$	8.314
λ_A	-	1
λ_C	-	1
i_m	A cm^{-2}	2.5
β_2	-	2
Δh @90 °C	J mol^{-1}	-283900
Δh @100 °C	J mol^{-1}	-283700
P_{H_2} @90 °C	atm	0.8046
P_{H_2} @100 °C	atm	0.4952
P_{O_2} @90°C	atm	0.4061
P_{O_2} @100 °C	atm	0.3516
σ_{mem}@90 °C	cm Ω^{-1}	0.1770
σ_{mem}@100 °C	cm Ω^{-1}	0.1943
β_1@90 °C	-	0.3299
β_1@100 °C	-	0.3375
y@90 °C	-	0.369
y@100 °C	-	0.94
$\Theta_{G,ar}$	$Wm^{-2}K^{-1}$	1163
b_1	-	1
b_2	-	1
I_{ar}	-	1.05
T_o	K	313.15
$T_{L,ar}$	K	278.15